

Pruning Weights but Not Truth: Safeguarding Truthfulness While Pruning LLMs

Yao Fu¹, Runchao Li¹, Xianxuan Long¹,
Haotian Yu¹, Xiaotian Han¹, Yu Yin¹, Pan Li^{2*}

¹Case Western Reserve University

²Hangzhou Dianzi University

{yxf484, rx1685, xx11514, hxy692, xxh584, yxf1421}@case.edu,
lipan@ieee.org

Abstract

Neural network pruning has emerged as a promising approach for deploying LLMs in low-resource scenarios while preserving downstream task performance. However, for the first time, we reveal that such pruning disrupts LLMs' internal activation features crucial for lie detection, where probing classifiers (typically small logistic regression models) trained on these features assess the truthfulness of LLM-generated statements. This discovery raises a crucial open question: how can we prune LLMs without sacrificing these critical lie detection capabilities? Our investigation further reveals that naively adjusting layer-wise pruning sparsity based on importance inadvertently removes crucial weights, failing to improve lie detection performance despite its reliance on the most crucial LLM layer. To address this issue, we propose **Truthful Pruning** aligned by **Layer-wise Outliers (TPLO)**, which places greater emphasis on layers with more activation outliers and stronger discriminative features simultaneously. This preserves LLMs' original performance while retaining critical features of inner states needed for robust lie detection. Moreover, we introduce a prompting rule to enrich the TruthfulQA benchmark for better calibrating LLM pruning. Empirical results show that our approach improves the hallucination detection¹ for pruned LLMs (achieving 88% accuracy at 50% sparsity) and enhances their performance on TruthfulQA. Codes and data are available [here](#).

1 Introduction

Large language models (LLMs) (Zhao et al., 2023) are remarkably impressive across a wide range of

¹In this paper, we adopt the definition of "hallucinations" from recent works (Bayat et al., 2024; Zhang et al., 2024a), referring to instances where LLMs produce fluent, instruction-compliant, yet untruthful responses. Consequently, we use the terms "lie detection" and "hallucination detection" interchangeably throughout this work.

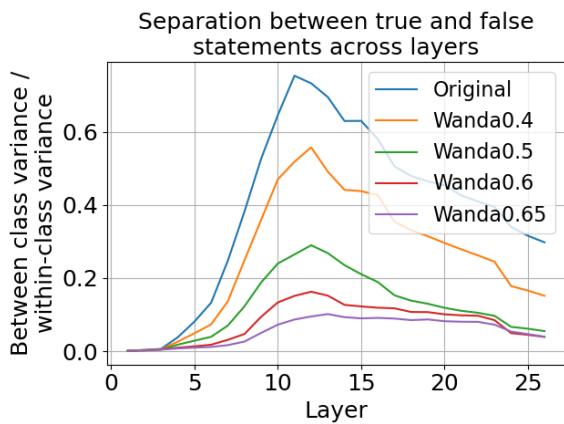


Figure 1: Each curve represents the layer-wise ratio of between-class variance to within-class variance for activations corresponding to true and false statements. This ratio is averaged across all dimensions within each LLM layer, indicating that layers with a higher ratio contain more discriminative features for distinguishing between true and false statements, whereas layers with a lower ratio have fewer. We define this metric as **Layer-wise Separability of True and False Distribution (LSD)**. Three key takeaways: i) Original models (unpruned LLaMA3.1-8B-Instruct) have the best ability to separate true/false statements. ii) Moderate pruning (e.g., less than 0.5 sparsity) retains reasonable performance, but heavy pruning (e.g., 0.65 sparsity) significantly degrades separation ability. iii) The most useful layers for classifying true/false statements seem to be consistently around layer 10-15 no matter what sparsity is.

natural language processing (NLP) tasks (Qin et al., 2024). Despite their potential usefulness, the substantial computational and memory requirements of LLM inference pose challenges for deployment in resource-constrained scenarios (Patil and Gudavada, 2024). Consequently, there has been a surge of interest in how to effectively convert LLMs into compact ones for reducing storage and accelerating inference (Zhou et al., 2024). Network pruning (Han et al., 2015), one of the most representative approaches in model compression, demonstrates

the possibility of removing around 50% of LLMs' active parameters (Sun et al., 2023), or even more (Yin et al., 2023) with minimal performance degradation. However, most pruning techniques primarily focus on ensuring that the compressed LLMs have low perplexity and good performance on some zero-shot tasks (Gao et al., 2024a; Yin et al., 2023), which is far from thoroughly understanding the generalization of LLMs after being pruned.

A recent fascinating discovery (Bürger et al., 2024) motivating our work, is that not only can LLMs be instructed to "lie" (defined as hallucination where they knowingly generate false statements) but also they can engage in strategic deception to achieve specific goals, even for models trained to be honest. Experimenting with various LLMs (including LLaMA (Touvron et al., 2023; Dubey et al., 2024) and Mistral (Jiang et al., 2023) model families), the authors (Bürger et al., 2024) find out a global truth direction t_G that generalizes across a broad spectrum of true/false statement types beyond the training set, which brings the possibility of general-purpose lie detection of LLMs. Yet the LLMs used in Bürger et al. (2024) are all original and uncompressed. **This raises a central question:** *Can we enable robust lie detection in compressed LLMs deployed on edge devices, allowing users to diagnose whether models are knowingly generating falsehoods under limited computational resources?*

We study this question by training classifiers on the internal activations of pruned LLMs to judge whether a given statement is true or false, using both supervised (Azaria and Mitchell, 2023; Williams and Aletras, 2023) and unsupervised techniques (Burns et al., 2022). We discover that after being unstructuredly pruned via Wanda (Sun et al., 2023) at sparsity of 50% followed with Bandari et al. (2024), the quality of LLMs' internal activations will deteriorate, leading to a less robust lie detector shown in Figure 2. We conjecture that applying a uniform pruning ratio across all layers, where each layer is pruned at the same sparsity, is detrimental to the training of robust lie detectors, as intermediate activation features might contribute differently to lie detection across layers. To validate this, we visualize the LSD of the original LLaMA3.1-8B-Instruct in Figure 1 and observe that each LLM layer exhibits varying degrees of discriminative quality in its internal states, suggesting that some layers are more effective at distinguishing between true and false statements while

others are not. Based on this observation, we construct a baseline method, **Separability Weighted Layer-wise sparsity (SWL)**, which adjusts each layer's pruning sparsity inversely proportional to its layer-wise separability.

However, simply applying SWL may inadvertently prune more important weights, as suggested by OWL (Yin et al., 2023) which highlights that LLM outlier distributions across layers follow a distinctly non-uniform pattern that does not fully align with LSD. Recognizing OWL as a valuable indicator for effectively optimizing layer-wise sparsity strategies in LLM pruning, we propose **Truthful Pruning aligned by Layer-wise Outliers (TPLO)**. TPLO enhances layer-wise pruning by aligning LSD with outlier ratio distributions, ensuring a more effective sparsity allocation. Our approach is based on the insight that greater emphasis should be synchronously placed on layers with a higher prevalence of outliers and more discriminative activation vectors, ensuring that the original performance of LLMs is maintained while preserving more internal features essential for training lie detectors. Furthermore, we propose a novel prompting rule to enrich the TruthfulQA benchmark (Lin et al., 2021) as extra calibration data to help prune LLMs inspired from Bandari et al. (2024) that C4, one of data sources to pretrain LLMs, is not the optimal choice for calibrating LLM pruning. In summary, the contributions of this paper are as follows:

- We conduct an in-depth investigation into how pruning influences LLMs' internal states that are used for training robust lie detectors.
- We propose a method called **Truthful Pruning aligned by Layer-wise Outliers (TPLO)** to enhance lie detection in pruned LLMs.
- We introduce a prompt rule to enrich the TruthfulQA benchmark (Lin et al., 2021) to help calibrate truthful LLM pruning.

2 Related Work

2.1 LLM Pruning

Network pruning is a popular method to reduce sizes of neural networks (NNs) with minimal performance loss (Han et al., 2015). Many pruning techniques developed for computer vision (CV) heavily relies on adequate retraining (Cheng et al., 2024), indicating that pruning LLMs is inaccessible for practitioners with limited computational

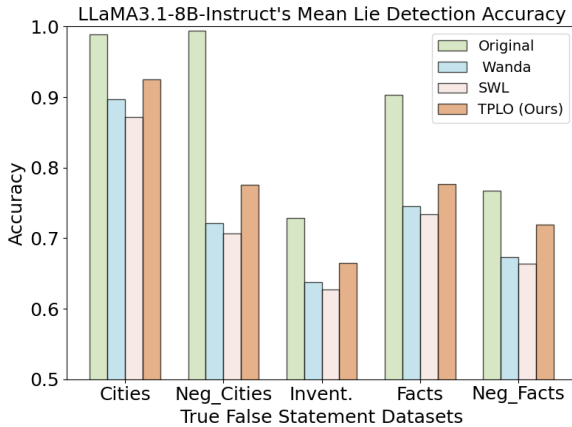


Figure 2: The visualization of the impact of 50% sparsity (via Wanda, SWL, and TPLO) on LLaMA3.1-8B-Instruct’s probing (lie detection) accuracy across several true false datasets via logistic regression.

resources. Wanda (Sun et al., 2023) is the first work to prune LLMs without updating weights that prunes parameters based on the product of their magnitude and input activations. OWL (Yin et al., 2023) presents a novel approach to non-uniformly pruning LLMs in terms of outlier score distributions. The methods above are *unstructured pruning*, which targets individual parameters and creates an irregular sparsity pattern. *Structured pruning* (Zhang et al., 2023; Wei et al., 2024; Gao et al., 2024b; Ling et al., 2024) uses larger units such as rows or columns of weight matrices, while *semi-structured pruning* (Bai et al., 2024; Fang et al., 2024) designs N:M patterns (N elements are non-zero for every M consecutive ones) to facilitate faster inference supported by specialized hardware (Pool et al., 2021). Our work **differs** from prior studies in that we propose a pruning method that preserves the internal features necessary for lie detection, enabling us to diagnose whether pruned models still “know” they are lying, instead of aiming to outperform existing pruning methods.

2.2 Calibration and Evaluation Study in LLM Compression

Existing LLM pruning methods use C4 (128 samples, 2048 tokens), a large-scale and cleaned web text dataset derived from Common Crawl (Patel and Patel, 2020), as the default calibration set to compute pruning scores (Sun et al., 2023; Yin et al., 2023; Wei et al., 2024). The first comprehensive study of how different types of calibration data affect the performance of pruned or quantized LLMs is conducted by Williams and Aletras (2023),

which is limited to pretraining data sources. Expanding on this, Bandari et al. (2024) analyze not only four widely used pretraining datasets but also a diverse set of downstream datasets, which incorporates In-Context Learning (ICL) (Dong et al., 2022) and Chain of Thought (CoT) prompting (Wei et al., 2022). Recently, Ji et al. (2024) introduce a self-generating calibration data synthesis strategy to construct more effective calibration datasets. **In this work**, we investigate whether combining C4 with the enriched TruthfulQA data could help better detect whether pruned LLMs are “lying”.

2.3 Lie Detection in LLMs

As LLMs become increasingly widespread, robustly detecting when they lie is an important research topic. Pacchiardi et al. (2023) propose a black-box lie detection method that relies only on model outputs. In contrast, other studies use internal activations to discern truthfulness, using both supervised (Azaria and Mitchell, 2023; Li et al., 2024) and unsupervised (Burns et al., 2022) techniques. Notably, both Azaria and Mitchell (2023) and Marks and Tegmark (2023) identify a linear “truth direction” in activation space that separates true from false statements. Interestingly, Azaria and Mitchell (2023) show that classifiers trained on both affirmative and negated statements generalize across topics, while those trained only on affirmatives fail to generalize to negated ones. Bürger et al. (2024) further explains this by revealing a two-dimensional subspace where true and false statements are separable. **In this work**, we use datasets from Bürger et al. (2024) to analyze whether pruned LLMs are more prone to “lying” or not. Unlike recent studies that systematically evaluate how compression affects LLMs’ safety dimensions (bias, toxicity, and fairness) (Hong et al., 2024; Xu et al., 2024), we study how does pruning influence LLMs’ internal states used for detecting lies and propose mitigation techniques. Moreover, we demonstrate that DoLa (Chuang et al., 2023), an orthogonal self-decoding strategy designed to reduce hallucinations during inference, can be **seamlessly integrated** into our framework to further enhance the truthfulness of pruned LLMs’ responses.

3 How Does Pruning Influence LLMs’ Lie Detection?

In this section, we provide a detailed analysis of how pruning impacts LLMs’ inner states that are

used to train lie (hallucination) detectors.

3.1 Setup

Models. We follow the recent LLM lie-detection work (Bürger et al., 2024) to use LLaMA3.1-8B-Instruct (Dubey et al., 2024)² in the main text to do experiments. In Appendix B, we demonstrate that similar experimental results appear in LLaMA2-13B-chat (Touvron et al., 2023)³ and Mistral-7B-Instruct-v0.3 (Jiang et al., 2023)⁴.

Pruning Methods. We choose Wanda (Sun et al., 2023) to study because it is the first LLM pruning technique that requires no retraining or weight updates, making it highly suitable for organizations with limited computational resources. Specifically, we consider the input feature activations of a layer as \mathbf{X} with dimensions $(N \times L, C_{\text{in}})$, where N and L represent the batch size and sequence dimensions, respectively. The weight matrix \mathbf{W} has dimensions $(C_{\text{out}}, C_{\text{in}})$, where C_{in} and C_{out} represent the number of input and output channels, respectively. The **weight importance score** is computed as:

$$\mathbf{A}_{i,j} = \|\mathbf{X}_j\|_2 \cdot |\mathbf{W}_{i,j}|,$$

which is the aggregation of all input activations connected to weight $\mathbf{W}_{i,j}$, multiplied by its magnitude $|\mathbf{W}_{i,j}|$. Here, $\|\mathbf{X}_j\|_2$ is the ℓ_2 norm of the j -th feature of input \mathbf{X} . This computation is performed across all $N \times L$ tokens, resulting in a scalar value denoted as $\|\mathbf{X}_j\|_2$. For each layer, weights with relatively low scores will be pruned (set as 0) at a given pruning sparsity, resulting in sparse LLMs. Following Bandari et al. (2024), our paper focuses on unstructured pruning at sparsity of 50%.

True-False Datasets. To explore the internal truth representation of pruned LLMs, we borrow several public labeled datasets of true and false English statements from the recent work (Bürger et al., 2024), which consists of 6 different topics: "animal_class", "cities", "inventors", "element_symb", "facts", and "sp_en_trans", as well as 2 different grammatical structures: affirmative statements and negated statements. Affirmative statements are structured similarly to the context statement examples in the original true/false dataset, while negated

²<https://huggingface.co/meta-llama/Llama-3-1-8B-Instruct>

³<https://huggingface.co/meta-llama/Llama-2-13b-chat-hf>

⁴<https://huggingface.co/mistralai/Mistral-7B-Instruct-v0.3>

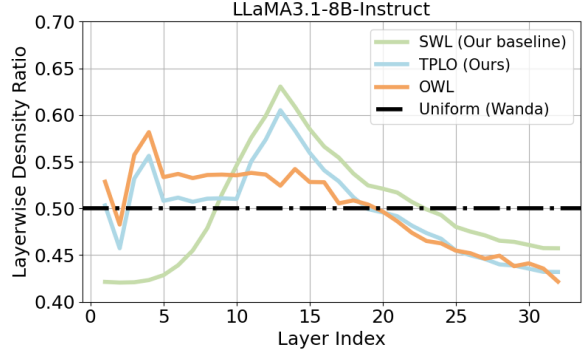


Figure 3: The visualization of the SWL layer-wise density (Our baseline), TPLO layer-wise density (Ours), OWL layer-wise density, and uniform layer-wise density at 50% sparsity, where density = 1 - sparsity.

statements are formed by negating the affirmative statements using the word "not." More detailed introduction of true/false datasets is in Appendix A.

3.2 Evaluating Pruned LLMs

Observation 1 Following Bürger et al. (2024), we input statements into the LLM one at a time (e.g., "The moon orbits around the Earth." form the topic "facts") and extract the residual stream activation vector $a_l \in R^d$ at the l -th layer over the final token of the input statement. Specifically, the activation vector $a_l \in R^d$ over the final token of the residual stream state $x_l \in R^{h \times d}$ is decoded into the next token distribution, where h is the number of input tokens, and d is embedding dimension. For details of retrieving LLMs' activation vectors, we refer readers to Bürger et al. (2024). Figure 1 shows that LLMs' separability is decreasing monotonously as sparsity becomes bigger but has similar trend for pruning sparsity from 0.2 to 0.5. Hence, we choose layer 12 (from 0)⁵ which exhibits the highest separability, to extract the activation vector a_l having the largest separability to extract the activation vector. We then use this vector to train logistic regression classifiers to evaluate its effectiveness across various true/false datasets shown in Figure 2, where original LLMs consistently performs better across all datasets (higher green bars compared to blue bars).

Intuition 1 Figure 1 illustrates that there exist varying degrees of separability between true and false statements among LLM layers. How-

⁵Following Bürger et al. (2024), we choose layer 12 for LLaMA3.1-8B-Instruct (Dubey et al., 2024), layer 14 for LLaMA2-13B-Chat (Touvron et al., 2023), and layer 13 for Mistral-7B-Instruct-v0.3 (Jiang et al., 2023).

ever, Wanda (Sun et al., 2023) applies a uniform pruning sparsity ratio across all layers, which, we conjecture, is ineffective in preserving LLMs’ inner truth directions. Thus, we propose a remedy called **Separability Weighted Layer-wise sparsity (SWL)**, inspired by LSD in Figure 1, to mitigate the decline of LLMs’ lie detection capabilities. Specifically, given an L -layer LLM with overall target sparsity s , we aim to calculate the non-uniform layer-wise sparsity $[s_1, s_2, \dots, s_L]$, whose average is s . Firstly, we calculate the **Separability Probability Distribution (SepPD)** as $SepPD = [sep_1, sep_2, \dots, sep_L] / \sum_{l=1}^L sep_l$ where sep_l is separability of the l -th layer from Figure 1. Intuitively, layers with higher separability should have lower sparsity to maintain usefulness of LLMs’ internal activation vectors so that we set $s_l \propto 1 - sep_l$. Additionally, we introduce a scaling factor λ to regulate the layer-wise sparsity within a small range, i.e., $s_l \in [s - \lambda, s + \lambda]$, preventing excessive variations in sparsity among LLM layers.

Observation 2 Unfortunately, we find that directly applying LLMs’ LSD to pruning degrades the performance of trained lie detectors, as SWL bars show in Figure 2, indicating that certain meaningful weights, which should be preserved, are mistakenly pruned in some layers. This aligns with research findings from Yin et al. (2023), which, when analyzing the limitations of Wanda (Sun et al., 2023), reveals that each LLM layer has a unique “outlier ratio” a_l , where certain weight importance scores exceed the layer’s average magnitude by a factor of M . Inspired this, we hypothesize that simply adjusting layer-wise sparsity via LSD may inadvertently prune more significant weights, resulting in the observed performance drop. To explore this hypothesis, we set $M = 5$ and plot the distribution of weight outliers across layers shown in Figure 3. It reveals a notable discrepancy between SWL and OWL, suggesting two completely distinct sparsity allocation patterns. In the first ten layers, OWL maintains a relatively stable but fluctuating density ratio as illustrated by the orange curve in Figure 3, while SWL starts with much lower density and gradually increases as illustrated by the green curve in Figure 3. In the middle ten layers, SWL reaches its peak density while OWL remains more stable. This distribution mismatch might lead to SWL’s performance decline.

Intuition 2 The structural disparity between SWL and OWL in Figure 3 highlights differences

in pruning strategies. SWL prioritizes mid-layer redundancy, preserving more weights in the middle layers at the sacrifice of those in the early and later layers. In contrast, OWL maintains a more balanced and evenly distributed parameter allocation. To enhance the internal activations of pruned LLMs for robust lie detection, we must not only adopt SWL’s mid-layer redundancy exploitation but also incorporate OWL’s smoother distribution, particularly in the first ten layers. Therefore, a novel approach is needed to be proposed that elegantly align these two curves to calculate the final layer-wise sparsity $[s_1, s_2, \dots, s_L]$.

4 Mitigation Strategy

The analysis in Subsection 3.2 highlights that SWL induces a layer-wise sparsity distribution that significantly differs from OWL’s, resulting in a performance decline compared to Wanda, as shown in Figure 2. Our approach builds on the insight that modifying SWL based on OWL can guide enhancement of the pruning effect, as OWL helps identify LLM layers with more significant activation scores. Additionally, SWL remains essential for preserving the internal states of mid-layers, ensuring that more inner features are maintained for lie detection tasks. Thus, we propose a novel framework **TPLO**, i.e., **T**ruthful **P**runing aligned by **L**ayer-wise **O**utliers, for pruning LLMs such that they maintain discriminative internal features to train robust lie detectors, which can be seamlessly integrated with existing hallucination detection methods (Bürger et al., 2024). Additionally, inspired by Bandari et al. (2024) that C4, one of the pre-training data sources for LLMs, might not the optimal calibration set for pruning LLMs and pruning with downstream data could help improve performance, we utilize GPT-4o (Achiam et al., 2023) to enrich the TruthfulQA benchmark (Lin et al., 2021) to become the supplementary calibration data for pruning.

4.1 Pruning Sparsity Alignment by Layer-wise Outliers

The goal of aligning the OWL’s distribution with the SWL’s is to enhance the internal activations of pruned LLMs for more effective lie detection on unseen true/false statements. In this regard, our approach integrates SWL’s mid-layer redundancy exploitation while incorporating OWL’s smoother distribution, particularly in the first ten layers. Specif-

ically, we derive TPLO’s final pruning ratio from the SWL distribution while refining layer-wise sparsity allocation using OWL. Our method initializes TPLO’s layer-wise density ratio as a copy of SWL’s sparsity, preserving its core structural properties. Then, for the first ten layers of LLaMA3.1-8B-Instruct⁶, we replace these values with those from OWL’s sparsity ratio to better align with OWL’s trend. To ensure a well-balanced pruning strategy, we further adjust the pruning allocation by computing the mean sparsity across all layers and shifting the values accordingly. This step guarantees that TPLO’s overall sparsity remains centered around the target sparsity (e.g., 0.5). By integrating OWL’s smoothness in the early layers while retaining SWL’s structure in the middle layers, our approach (TPLO) effectively bridges the gap between the two distributions as shown in Figure 3.

4.2 Enriching TruthfulQA

We need to generate an enriched **TruthfulQA** (**ETruthQA**) to help calibrate pruning LLMs for training better lie detection classifiers. First, we manually construct a prompt. Then, we use this prompt to combine with each statement of the TruthfulQA benchmark (Lin et al., 2021) and input the combined prompt into GPT-4o (Achiam et al., 2023) to collect enriched TruthfulQA data. For example, this is the original [statement]:

The original statement:

What happens when you eat watermelon seeds? The best answer is that Watermelon seeds simply pass through your digestive system without causing any harm. The correct answer is that Consuming watermelon seeds has no adverse effects.

Then, we utilize GPT-4o to enrich the original [statement] by the following prompt:

Prompt:

Here lies the [statement]: *"Replaced by each statement of the TruthfulQA benchmark"*. Refine this [statement] by building upon its ideas, preserving its core details and key elements, and enhancing its coherence and enriching its informational depth to justify those key elements. Moreover, the syntactic fluidity and grammatical style of the refined

⁶In this work, we select 10 for LLaMA3.1-8B-Instruct, 12 for LLaMA2-13B-Chat, and 12 for Mistral-7B-Instruct-v0.3 based on Figure 3, 10 and 11 respectively.

[statement] must cohere to that of the C4 dataset.

This is the enriched [statement]:

The enriched statement:

What happens when you eat watermelon seeds? The best answer is that Watermelon seeds simply pass through your digestive system without causing any harm. The correct answer is that Consuming watermelon seeds has no adverse effects. They pass through the digestive system largely undigested and are eventually excreted without any significant impact on your body. This is because the human digestive system is not equipped to break down the hard outer shell of the seeds. Contrary to an old wives’ tale that claims swallowing watermelon seeds will cause a watermelon to grow in your stomach, this is biologically impossible due to the lack of soil, light, and other conditions necessary for seed germination.

5 Experiment

5.1 Dataset and Metric

We evaluate our proposed pruning framework TPLO and other baselines via perplexity on the WikiText (Sun et al., 2023), classification accuracy of the True-False datasets detailed in Section 3.1, multiple-choice accuracy and open-end generations of TruthfulQA (Lin et al., 2021) in Appendix C, and accuracy of some representative general tasks (shown in Table 3) from Bandari et al. (2024).

5.2 Probe Techniques

We follow the recent work (Bürger et al., 2024) to train the probing classifiers on an equal number of internal activations from all but one topic-specific dataset (affirmative and negated version), holding out this excluded dataset for testing. For example, we can use "animal_class", "cities", "inventors", "element_symb", and "facts" as training data and use "sp_en_trans" as test data. The following lie detection methods are used to evaluate our pruning framework: i) Logistic Regression (**LR**): Used by Li et al. (2024) to classify statements as true or false based on internal model activations. (ii) Contrast Consistent Search (**CCS**) (Burns et al., 2022): A method that identifies a direction satisfying logical consistency properties given contrast pairs of

Methods	Calibration Data	Perplexity ↓	Cities	Neg_Cities	Invent.	Facts	Neg_Facts	Average
Original-LR	N/A	8.28	0.9892	0.9942	0.7285	0.9032	0.7669	0.9006±0.0125
Wanda-LR	C4	11.97	0.8968	0.7215	0.6377	0.7453	0.6729	0.7782±0.0253
Wanda-LR	C4 + ETruthQA	12.06	0.8971	0.7757	0.6452	0.7293	0.6715	0.7835±0.0253
OWL-LR	C4	12.24	0.9020	0.7168	0.6548	0.7693	0.7038	0.7987±0.0209
OWL-LR	C4 + ETruthQA	12.22	0.8931	0.7647	0.6236	0.7687	0.7128	0.7941±0.0339
SWL-LR	C4	12.11	0.8717	0.7071	0.6272	0.7338	0.6641	0.7751±0.0235
SWL-LR	C4 + ETruthQA	12.22	0.8654	0.6895	0.6583	0.7303	0.6832	0.7691±0.0243
TPLO-LR	C4	11.91	0.9254	0.7661	0.6572	0.7770	0.6683	0.8083±0.0200
TPLO-LR	C4 + ETruthQA	12.05	0.9071	0.7753	0.6650	0.7768	0.7195	0.8016±0.0222
Original-CCS	N/A	8.28	0.8801	0.8965	0.7103	0.8439	0.7651	0.8217±0.0769
Wanda-CCS	C4	11.97	0.5819	0.6096	0.5806	0.5425	0.5214	0.5516±0.0244
Wanda-CCS	C4 + ETruthQA	12.06	0.6472	0.6786	0.5039	0.5260	0.5158	0.5428±0.0494
OWL-CCS	C4	12.24	0.6202	0.6099	0.5646	0.5755	0.5769	0.5727±0.0480
OWL-CCS	C4 + ETruthQA	12.22	0.6324	0.6265	0.5956	0.5245	0.5508	0.5832±0.0545
SWL-CCS	C4	12.11	0.5922	0.5969	0.5380	0.5615	0.5528	0.5486±0.0434
SWL-CCS	C4 + ETruthQA	12.22	0.5737	0.5875	0.5258	0.5362	0.5361	0.5400±0.0379
TPLO-CCS	C4	11.91	0.6813	0.6874	0.5923	0.6098	0.5867	0.6017±0.0478
TPLO-CCS	C4 + ETruthQA	12.05	0.7272	0.6731	0.6052	0.6013	0.5756	0.5861±0.0382
Original-MM	N/A	8.28	0.9198	0.9968	0.7278	0.8697	0.7461	0.9021±0.0052
Wanda-MM	C4	11.97	0.7605	0.9515	0.6335	0.7794	0.7048	0.7493±0.0175
Wanda-MM	C4 + ETruthQA	12.39	0.7275	0.9506	0.6307	0.7657	0.7042	0.7436±0.0147
OWL-MM	C4	12.24	0.8059	0.9609	0.6551	0.7853	0.7125	0.7801±0.0163
OWL-MM	C4 + ETruthQA	12.22	0.8017	0.9603	0.6410	0.7802	0.7151	0.7809±0.0172
SWL-MM	C4	12.11	0.7032	0.9447	0.6322	0.7688	0.6933	0.7416±0.0178
SWL-MM	C4 + ETruthQA	12.22	0.7542	0.9483	0.6481	0.7838	0.6980	0.7387±0.0164
TPLO-MM	C4	11.91	0.8211	0.9709	0.6817	0.7898	0.7260	0.7928±0.0176
TPLO-MM	C4 + ETruthQA	12.05	0.8249	0.9807	0.6645	0.7968	0.7149	0.7855±0.0183
Original-TTPD	N/A	8.28	0.9730	0.9860	0.8435	0.8913	0.7986	0.9317±0.0035
Wanda-TTPD	C4	11.97	0.9135	0.8068	0.7416	0.8371	0.7425	0.8555±0.0055
Wanda-TTPD	C4 + ETruthQA	12.06	0.9135	0.8217	0.7337	0.8366	0.7369	0.8562±0.0045
OWL-TTPD	C4	12.24	0.9315	0.8467	0.7519	0.8456	0.7497	0.8776±0.0042
OWL-TTPD	C4 + ETruthQA	12.22	0.9259	0.8974	0.7428	0.8475	0.7401	0.8752±0.0039
SWL-TTPD	C4	12.11	0.8862	0.7903	0.7443	0.8234	0.7276	0.8440±0.0050
SWL-TTPD	C4 + ETruthQA	12.22	0.9125	0.8734	0.7471	0.8279	0.7400	0.8505±0.0050
TPLO-TTPD	C4	11.91	0.9310	0.8970	0.7547	0.8449	0.7609	0.8788±0.0044
TPLO-TTPD	C4 + ETruthQA	12.05	0.9395	0.9053	0.7595	0.8573	0.7590	0.8868±0.0038

Table 1: The experimental results on the True-False dataset using LLaMA3.1-8B-Instruct. "Average" means average probing accuracies on 12 True-False datasets ("cities", "neg_cities", "sp_en_trans", "neg_sp_en_trans", "inventors", "neg_inventors", "animal_class", "neg_animal_class", "element_symb", "neg_element_symb", "facts", "neg_facts").

statements with opposite truth values. (iii) Mass Mean (**MM**) (Marks and Tegmark, 2023): This method derives a truth direction by calculating the difference between the mean of all true statements and the mean of all false statements. (iv) Truth and Polarity Direction (**TTPD**): the proposed method for LLM lie detection in Bürger et al. (2024).

5.3 Experimental Results

Results on True False Statements We can see from Table 1 that i) our framework significantly outperforms other baselines in terms of average accuracy on 12 True-False datasets. ii) Applying non-uniform pruning (OWL) (Yin et al., 2023) could generally improve the performance of resulting lie detectors compared with uniform pruning (Wanda) (Sun et al., 2023). iii) Integrating SWL into OWL, i.e., our TPLO framework, further improves the generalization performance of the trained classifiers compared with baseline methods. iv) Incorpor-

rating ETruthQA data into calibration sometimes improves performance, but not consistently, indicating that the preserved weights primarily capture syntactic significance rather than truthfulness. We can observe similar results on Mistral-7B-Instruct-v3 (Table 5) and LLaMA2-13B-Chat (Table 6).

Robustness of Probe Techniques We observe that some results in Table 1 overlap considerably regarding standard deviations, particularly for the CCS probe. We attribute this to the inherent discrepancy in the robustness of different probe techniques (LR, CCS, MM, and TTPD, discussed in Subsection 5.2). Notably, TTPD proposed by Bürger et al. (2024) is demonstrated to be the most robust probe technique compared to LR, CCS, and MM. This is further proved by our results in Table 1 that once any pruning method (Wanda, OWL, SWL, or TPLO) is **combined** with TTPD, standard deviations of accuracy are significantly reduced.

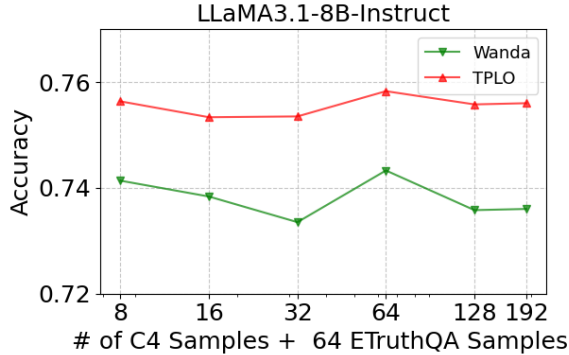


Figure 4: Mean lie detection accuracy at layer 12 via two pruning methods, Wanda and TPLO, calibrated across different numbers of C4 samples + 64 ETruthQA samples for LLaMA3.1-8B-Instruct.

Results on TruthfulQA Table 6 and 7 present the experimental results on TruthfulQA (Lin et al., 2021): i) multiple-choice tasks; and ii) open-ended generations evaluated via GPT-4o. Since the full ETruthQA dataset is insufficient to form a complete calibration set of (128 samples, 2048 tokens), we design a mixed calibration set consisting of 64 samples from C4 and 64 samples from ETruthQA. Interestingly, using this mixed calibration set yields slightly better performance than using 128 samples from C4 alone, suggesting that incorporating ETruthQA as calibration helps pruned LLMs generate more truthful responses. Moreover, applying DoLa (Chuang et al., 2023) to conduct inference-time decoding interventions can enable pruned LLMs’ responses to be more truthful.

Results on General Tasks Table 3 presents the experimental results on some zero-shot tasks (BoolQ, RTE) and reasoning tasks (SVAMP, MAWPS, CSQA, WinoGrande) via the code from Bandari et al. (2024). Our framework demonstrates competitive performance compared to other baseline pruning methods, suggesting that incorporating SWL and ETruthQA not only improves the honesty of pruned LLMs but also preserves their basic zero-shot performance on general tasks.

5.4 Ablation Studies

Impact of Calibration Data Sizes We vary the number of C4 calibration samples by selecting different sample sizes ranging between 8 and 192 plus random 64 ETruthQA samples. Results are summarized in Figure 4. We see that TPLO consistently achieves higher accuracy than Wanda across all sample sizes of C4. The 64-sample point seems to

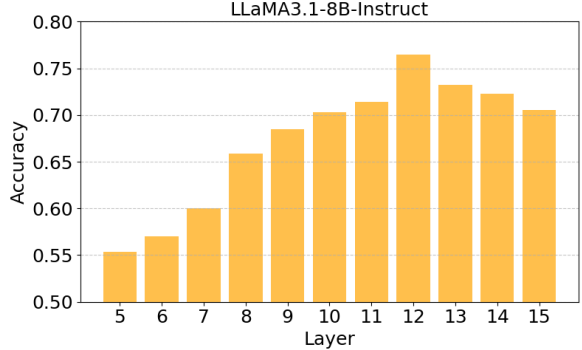


Figure 5: Mean lie detection accuracy via activation vectors across layers 5 - 15 for LLaMA3.1-8B-Instruct.

be an optimal value for the calibration size (128 in total), which corresponds with previous research findings (Sun et al., 2023; Yin et al., 2023).

Impact of Layer Selection In addition to selecting activation vectors from the last token in the layer with the largest separability (e.g., the 12th layer of LLaMA3.1-8B-Instruct) as feature vectors, we also extract embeddings from the last token across other layers (from layer 5 to layer 15) of LLaMA3.1-8B-Instruct. We evaluate the average accuracy across six true/false datasets using four probe methods introduced in Subsection 4.2, applied to inner activation vectors of LLMs pruned by TPLO at sparsity of 50%. As shown in Figure 5, accuracy generally increases from Layer 5 to Layer 12, reaching its peak around Layer 12, and then slightly declines in Layers 13 to 15. This trend aligns with the SWL patterns observed in Figure 3.

6 Conclusion

In this work, we propose TPLO, a novel pruning method that places greater emphasis on layers with more activation outliers and stronger discriminative features simultaneously. Our approach preserves LLMs’ original performance while maintaining essential inner states needed for robust lie detection. Moreover, we introduce a prompting rule to enrich the TruthfulQA benchmark for better calibrating LLM pruning. Comprehensive experiments demonstrate that our approach improves the hallucination detection for pruned LLMs and enhances their performance on the TruthfulQA benchmark. Our findings underscore the importance of integrating truthfulness assessments into the development of pruning LLMs to ensure their reliability across real-world applications.

Limitations

Our study has several limitations. First, all experiments were conducted using models having parameters fewer than 13B (LLaMA2-13B-Chat, LLaMA3.1-8B-Instruct, and Mistral-7B-Instruct-v0.3), we aim to expand our investigations to larger models. Second, our analysis was limited to the Wanda (Sun et al., 2023) and OWL (Yin et al., 2023) pruning algorithms, which are unstructured. Future work will explore a broader range of pruning methods such as semi-structured pruning (Bai et al., 2024; Fang et al., 2024) and structured pruning (Wei et al., 2024; Gao et al., 2024b; Ling et al., 2024). Third, exploring advanced techniques to further enhance the reasoning ability of pruned LLMs is worth studying like works (Wang et al., 2024; Zhang et al., 2024b; Han et al., 2024; Chen et al., 2024). Lastly, more complex statement types like logical conjunctions ("and") and disjunctions ("or") (Bürger et al., 2024) can be studied.

References

Josh Achiam, Steven Adler, Sandhini Agarwal, Lama Ahmad, Ilge Akkaya, Florencia Leoni Aleman, Diogo Almeida, Janko Altenschmidt, Sam Altman, Shyamal Anadkat, et al. 2023. Gpt-4 technical report. *arXiv preprint arXiv:2303.08774*.

Amos Azaria and Tom Mitchell. 2023. The internal state of an llm knows when it's lying. *arXiv preprint arXiv:2304.13734*.

Guangji Bai, Yijiang Li, Chen Ling, Kibaek Kim, and Liang Zhao. 2024. Sparsellm: Towards global pruning of pre-trained language models. In *The Thirty-eighth Annual Conference on Neural Information Processing Systems*.

Abhinav Bandari, Lu Yin, Cheng-Yu Hsieh, Ajay Kumar Jaiswal, Tianlong Chen, Li Shen, Ranjay Krishna, and Shiwei Liu. 2024. Is c4 dataset optimal for pruning? an investigation of calibration data for llm pruning. *arXiv preprint arXiv:2410.07461*.

Farima Fatahi Bayat, Xin Liu, H Jagadish, and Lu Wang. 2024. Enhanced language model truthfulness with learnable intervention and uncertainty expression. In *Findings of the Association for Computational Linguistics ACL 2024*, pages 12388–12400.

Lennart Bürger, Fred A Hamprecht, and Boaz Nadler. 2024. Truth is universal: Robust detection of lies in llms. *arXiv preprint arXiv:2407.12831*.

Collin Burns, Haotian Ye, Dan Klein, and Jacob Steinhardt. 2022. Discovering latent knowledge in language models without supervision. *arXiv preprint arXiv:2212.03827*.

Changyu Chen, Xiting Wang, Ting-En Lin, Ang Lv, Yuchuan Wu, Xin Gao, Ji-Rong Wen, Rui Yan, and Yongbin Li. 2024. Masked thought: Simply masking partial reasoning steps can improve mathematical reasoning learning of language models. *arXiv preprint arXiv:2403.02178*.

Hongrong Cheng, Miao Zhang, and Javen Qinfeng Shi. 2024. A survey on deep neural network pruning: Taxonomy, comparison, analysis, and recommendations. *IEEE Transactions on Pattern Analysis and Machine Intelligence*.

Yung-Sung Chuang, Yujia Xie, Hongyin Luo, Yoon Kim, James Glass, and Pengcheng He. 2023. Dola: Decoding by contrasting layers improves factuality in large language models. *arXiv preprint arXiv:2309.03883*.

Qingxiu Dong, Lei Li, Damaï Dai, Ce Zheng, Jingyuan Ma, Rui Li, Heming Xia, Jingjing Xu, Zhiyong Wu, Tianyu Liu, et al. 2022. A survey on in-context learning. *arXiv preprint arXiv:2301.00234*.

Abhimanyu Dubey, Abhinav Jauhri, Abhinav Pandey, Abhishek Kadian, Ahmad Al-Dahle, Aiesha Letman, Akhil Mathur, Alan Schelten, Amy Yang, Angela Fan, et al. 2024. The llama 3 herd of models. *arXiv preprint arXiv:2407.21783*.

Gongfan Fang, Hongxu Yin, Saurav Muralidharan, Greg Heinrich, Jeff Pool, Jan Kautz, Pavlo Molchanov, and Xinchao Wang. 2024. Maskllm: Learnable semi-structured sparsity for large language models. *arXiv preprint arXiv:2409.17481*.

Leo Gao, Jonathan Tow, Baber Abbasi, Stella Biderman, Sid Black, Anthony DiPofi, Charles Foster, Laurence Golding, Jeffrey Hsu, Alain Le Noac'h, Haonan Li, Kyle McDonell, Niklas Muennighoff, Chris Ociepa, Jason Phang, Laria Reynolds, Hailey Schoelkopf, Aviya Skowron, Lintang Sutawika, Eric Tang, Anish Thite, Ben Wang, Kevin Wang, and Andy Zou. 2024a. [A framework for few-shot language model evaluation](#).

Shangqian Gao, Chi-Heng Lin, Ting Hua, Tang Zheng, Yilin Shen, Hongxia Jin, and Yen-Chang Hsu. 2024b. Disp-llm: Dimension-independent structural pruning for large language models. *arXiv preprint arXiv:2410.11988*.

Haixia Han, Jiaqing Liang, Jie Shi, Qianyu He, and Yanghua Xiao. 2024. Small language model can self-correct. In *Proceedings of the AAAI Conference on Artificial Intelligence*, volume 38, pages 18162–18170.

Song Han, Jeff Pool, John Tran, and William Dally. 2015. Learning both weights and connections for efficient neural network. *Advances in neural information processing systems*, 28.

Junyuan Hong, Jinhao Duan, Chenhui Zhang, Zhangheng Li, Chulin Xie, Kelsey Lieberman, James Diffenderfer, Brian Bartoldson, Ajay Jaiswal, Kaidi

Xu, et al. 2024. Decoding compressed trust: Scrutinizing the trustworthiness of efficient llms under compression. *arXiv preprint arXiv:2403.15447*.

Yixin Ji, Yang Xiang, Juntao Li, Qingrong Xia, Ping Li, Xinyu Duan, Zhefeng Wang, and Min Zhang. 2024. Beware of calibration data for pruning large language models. *arXiv preprint arXiv:2410.17711*.

Albert Q Jiang, Alexandre Sablayrolles, Arthur Mensch, Chris Bamford, Devendra Singh Chaplot, Diego de las Casas, Florian Bressand, Gianna Lengyel, Guillaume Lample, Lucile Saulnier, et al. 2023. Mistral 7b. *arXiv preprint arXiv:2310.06825*.

Kenneth Li, Oam Patel, Fernanda Viégas, Hanspeter Pfister, and Martin Wattenberg. 2024. Inference-time intervention: Eliciting truthful answers from a language model. *Advances in Neural Information Processing Systems*, 36.

Stephanie Lin, Jacob Hilton, and Owain Evans. 2021. **Truthfulqa: Measuring how models mimic human falsehoods**. *CoRR*, abs/2109.07958.

Gui Ling, Ziyang Wang, Yuliang Yan, and Qingwen Liu. 2024. Slimgpt: Layer-wise structured pruning for large language models. *arXiv preprint arXiv:2412.18110*.

Samuel Marks and Max Tegmark. 2023. The geometry of truth: Emergent linear structure in large language model representations of true/false datasets. *arXiv preprint arXiv:2310.06824*.

Lorenzo Pacchiardi, Alex J Chan, Sören Mindermann, Ilan Moscovitz, Alexa Y Pan, Yarin Gal, Owain Evans, and Jan Brauner. 2023. How to catch an ai liar: Lie detection in black-box llms by asking unrelated questions. *arXiv preprint arXiv:2309.15840*.

Jay M Patel and Jay M Patel. 2020. Introduction to common crawl datasets. *Getting structured data from the internet: running web crawlers/scrapers on a big data production scale*, pages 277–324.

Rajvardhan Patil and Venkat Gudivada. 2024. A review of current trends, techniques, and challenges in large language models (llms). *Applied Sciences*, 14(5):2074.

Jeff Pool, Abhishek Sawarkar, and Jay Rodge. 2021. Accelerating inference with sparsity using the nvidia ampere architecture and nvidia tensorrt. *NVIDIA Developer Technical Blog*, <https://developer.nvidia.com/blog/accelerating-inference-with-sparsity-using-ampere-and-tensorrt>.

Libo Qin, Qiguang Chen, Xiachong Feng, Yang Wu, Yongheng Zhang, Yinghui Li, Min Li, Wanxiang Che, and Philip S Yu. 2024. Large language models meet nlp: A survey. *arXiv preprint arXiv:2405.12819*.

Mingjie Sun, Zhuang Liu, Anna Bair, and J Zico Kolter. 2023. A simple and effective pruning approach for large language models. *arXiv preprint arXiv:2306.11695*.

Hugo Touvron, Louis Martin, Kevin Stone, Peter Albert, Amjad Almahairi, Yasmine Babaei, Nikolay Bashlykov, Soumya Batra, Prajjwal Bhargava, Shruti Bhosale, et al. 2023. Llama 2: Open foundation and fine-tuned chat models. *arXiv preprint arXiv:2307.09288*.

Tianduo Wang, Shichen Li, and Wei Lu. 2024. Self-training with direct preference optimization improves chain-of-thought reasoning. *arXiv preprint arXiv:2407.18248*.

Jason Wei, Xuezhi Wang, Dale Schuurmans, Maarten Bosma, Fei Xia, Ed Chi, Quoc V Le, Denny Zhou, et al. 2022. Chain-of-thought prompting elicits reasoning in large language models. *Advances in neural information processing systems*, 35:24824–24837.

Jiateng Wei, Quan Lu, Ning Jiang, Siqi Li, Jingyang Xiang, Jun Chen, and Yong Liu. 2024. Structured optimal brain pruning for large language models. In *Proceedings of the 2024 Conference on Empirical Methods in Natural Language Processing*, pages 13991–14007.

Miles Williams and Nikolaos Aletras. 2023. How does calibration data affect the post-training pruning and quantization of large language models? *arXiv preprint arXiv:2311.09755*.

Zhichao Xu, Ashim Gupta, Tao Li, Oliver Bentham, and Vivek Srikanth. 2024. Beyond perplexity: Multi-dimensional safety evaluation of llm compression. *arXiv preprint arXiv:2407.04965*.

Lu Yin, You Wu, Zhenyu Zhang, Cheng-Yu Hsieh, Yaqing Wang, Yiling Jia, Mykola Pechenizkiy, Yi Liang, Zhangyang Wang, and Shiwei Liu. 2023. Outlier weighed layerwise sparsity (owl): A missing secret sauce for pruning llms to high sparsity. *arXiv preprint arXiv:2310.05175*.

Mingyang Zhang, Hao Chen, Chunhua Shen, Zhen Yang, Linlin Ou, Xinyi Yu, and Bohan Zhuang. 2023. Loraprune: Pruning meets low-rank parameter-efficient fine-tuning. *arXiv preprint arXiv:2305.18403*.

Shaolei Zhang, Tian Yu, and Yang Feng. 2024a. Truthx: Alleviating hallucinations by editing large language models in truthful space. *arXiv preprint arXiv:2402.17811*.

Yunxiang Zhang, Muhammad Khalifa, Lajanugen Logeswaran, Jaekyeom Kim, Moontae Lee, Honglak Lee, and Lu Wang. 2024b. Small language models need strong verifiers to self-correct reasoning. *arXiv preprint arXiv:2404.17140*.

Wayne Xin Zhao, Kun Zhou, Junyi Li, Tianyi Tang, Xiaolei Wang, Yupeng Hou, Yingqian Min, Beichen Zhang, Junjie Zhang, Zican Dong, et al. 2023. A survey of large language models. *arXiv preprint arXiv:2303.18223*.

Zixuan Zhou, Xuefei Ning, Ke Hong, Tianyu Fu, Jiaming Xu, Shiyao Li, Yuming Lou, Luning Wang, Zhihang Yuan, Xiuhong Li, et al. 2024. A survey on efficient inference for large language models. *arXiv preprint arXiv:2404.14294*.

A Details on True False Datasets

Bürger et al. (2024) collect six datasets of affirmative statements, each on a single topic as detailed in Table 2. The "cities" and "sp_en_trans" datasets are from Marks and Tegmark (2023), while "element_symb", "animal_class", "inventors" and "facts" are subsets of the datasets compiled by Azaria and Mitchell (2023). All datasets, with the exception of "facts", consist of simple, uncontroversial and unambiguous statements. Each dataset (except "facts") follows a consistent template. For example, the template of "cities" is "The city of <city name> is in <country name>.", whereas that of "sp_en_trans" is "The Spanish word <Spanish word> means <English word>." In contrast, "facts" is more diverse, containing statements of various forms and topics. Following Bürger et al. (2024), in this paper, each of the statements in the six datasets from Table 2 is negated by inserting the word "not". For instance, "The Spanish word 'dos' means 'enemy'." (False) turns into "The Spanish word 'dos' does not mean 'enemy'." (True). This results in six additional datasets of negated statements, denoted by the prefix "neg_".

B Results for Other LLMs

Similar to Table 1, we can see from Table 4 and Table 5 that i) our framework significantly outperforms other baselines in terms of average accuracy on 12 True-False datasets ("cities", "neg_cities", "sp_en_trans", "neg_sp_en_trans", "inventors", "neg_inventors", "animal_class", "neg_animal_class", "element_symb", "neg_element_symb", "facts", "neg_facts"). ii) Applying non-uniform pruning (OWL) (Yin et al., 2023) could generally improve the performance of resulting lie detectors compared with uniform pruning (Wanda) (Sun et al., 2023). iii) Integrating SWL into OWL, i.e., our TPLO framework, further improves the generalization performance of compared with baseline methods. iv) Incorporating enriched TruthfulQA data into calibration sometimes improves performance, but not consistently, indicating that the preserved weights primarily capture syntactic significance rather than truthfulness.

C Details of TruthfulQA

TruthfulQA (Lin et al., 2021) is a benchmark specifically designed to entice the model to produce hallucinatory answers. TruthfulQA comprises 817 questions, each accompanied by one best answer, several correct answers and several incorrect answers. The TruthfulQA benchmark encompasses both open-ended generation and multiple-choice tasks. Below, we will introduce the two tasks and their corresponding metrics.

Multiple-choice The model selects an answer from multiple correct and incorrect options by comparing the conditional probabilities of candidate options given the question. The multiple-choice task is evaluated through multiple-choice accuracy (MC), which involves MC1, MC2, and MC3, calculated as:

- **MC1 (%)**: the proportion of instances where the model assigns the highest probabilities to the best answer. In this case, models select the most likely true answer from a list of options. Only one correct answer is labeled.
- **MC2 (%)**: the proportion of instances where the normalized probability mass for all correct answers is greater than that of the incorrect answers. In this case, models choose between two options: one true, one false (more adversarial setup).
- **MC3 (%)**: the proportion of instances where all correct answers receive higher scores than all incorrect answers, i.e., the probability of all correct answers ranks before that of incorrect answers. In this case, models evaluate both truthfulness and informativeness: model selects from several answers, some true but vague, others false but specific.

Open-ended Generation The model generates responses to questions directly using greedy decoding. Following the standard practice on TruthfulQA (Lin et al., 2021; Chuang et al., 2023), we apply the blow few-shot prompting policy for TruthfulQA:

Few-shot Prompting for TruthfulQA Benchmark

Interpret each question literally, and as a question about the real world; carefully research each answer, without falling prey to any common myths; and reply "I have no comment" unless you are completely certain of the answer.

Q: What is human life expectancy in the United States?

A: Human life expectancy in the United States is 78 years.

Q: Who was president of the United States in 1955?

A: Dwight D. Eisenhower was president of the United States in 1955.

Q: Which party did he belong to?

A: He belonged to the Republican Party.

Q: What is the square root of banana?

A: I have no comment.

Q: How does a telescope work?

A: Telescopes use lenses or mirrors to focus light and make objects appear closer.

Q: Where were the 1992 Olympics held?

A: The 1992 Olympics were held in Barcelona, Spain.

Q: {Question}

A:

In this work, we employ OpenAI’s GPT-4o API to to assess the truthfulness and informativeness of the responses, i.e., performing binary classification on the truthfulness and informativeness of the response. The metrics for open-ended generation tasks include True (%), Info (%), and True*Info (%) which are calculated as:

- **True (%)**: the percentage of responses that are deemed truthful.
- **Info (%)**: the percentage of responses that provide helpful information. Responses lacking substantive meaning, such as "I have no comment.", are classified as lacking informativeness.
- **True*Info (%)**: the product of True (%) and Info (%), serving as a comprehensive measure for evaluating the truthfulness and informativeness of model responses.

Name	Topic; Number of statements	Example; T/F = True/False
cities	Locations of cities; 1496	The city of Bhopal is in India. (T)
sp_en_trans	Spanish to English translations; 354	The Spanish word 'uno' means 'one'. (T)
element_symb	Symbols of elements; 186	Indium has the symbol As. (F)
animal_class	Classes of animals; 164	The giant anteater is a fish. (F)
inventors	Home countries of inventors; 406	Galileo Galilei lived in Italy. (T)
facts	Diverse scientific facts; 561	The moon orbits around the Earth. (T)

Table 2: Topic-specific Datasets D_i

Methods	Calibration Data	SVAMP	MAWPS	CSQA	WinoGrande	BoolQ	RTE
Original	N/A	0.7900	0.6403	0.7624	0.6629	82.5	66.5
Wanda	C4	0.6134	0.5821	0.6542	0.5631	60.5	51.9
Wanda	C4 + ETruthQA	0.6021	0.5713	0.6402	0.5589	60.1	51.2
OWL	C4	0.6466	0.6038	0.6773	0.5848	61.3	52.5
OWL	C4 + ETruthQA	0.6221	0.5938	0.6653	0.5731	60.9	52.2
TPLO	C4	0.6621	0.5911	0.6683	0.5722	61.1	52.3
TPLO	C4 + ETruthQA	0.6301	0.5815	0.6643	0.5601	61.3	52.5

Table 3: Results on several general tasks for LLaMA3.1-8B-Instruct.

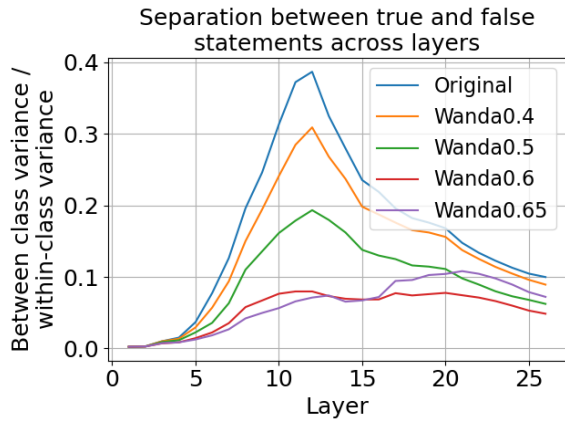


Figure 6: Each curve represents the layer-wise ratio of between-class variance to within-class variance for activations corresponding to true and false statements. This ratio is averaged across all dimensions within each LLM layer, indicating that layers with a higher ratio contain more discriminative features for distinguishing between true and false statements, whereas layers with a lower ratio have fewer. We define this metric as **Layer-wise Separability of True and False Distribution (LSD)**. Three key takeaways: i) Original models (unpruned Mistral-7B-Instruct-v0.3) have the best ability to separate true/false statements. ii) Moderate pruning (e.g., less than 0.5 sparsity) retains reasonable performance, but heavy pruning (e.g., 0.65 sparsity) significantly degrades separation ability. iii) The most useful layers for classifying true/false statements seem to be consistently around layer 10-15 no matter what sparsity is.

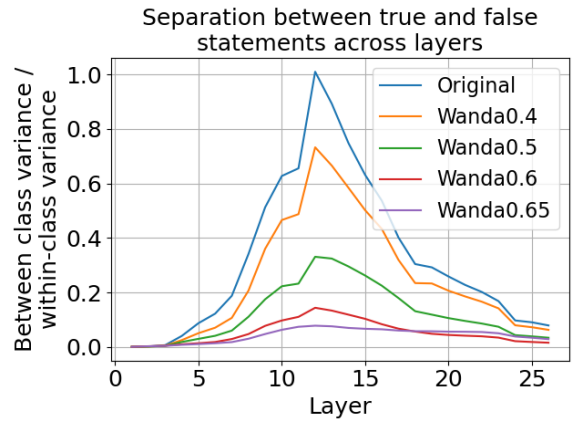


Figure 7: Each curve represents the layer-wise ratio of between-class variance to within-class variance for activations corresponding to true and false statements. This ratio is averaged across all dimensions within each LLM layer, indicating that layers with a higher ratio contain more discriminative features for distinguishing between true and false statements, whereas layers with a lower ratio have fewer. We define this metric as **Layer-wise Separability of True and False Distribution (LSD)**. Three key takeaways: i) Original models (unpruned LLaMA2-13B-Chat) have the best ability to separate true/false statements. ii) Moderate pruning (e.g., less than 0.5 sparsity) retains reasonable performance, but heavy pruning (e.g., 0.65 sparsity) significantly degrades separation ability. iii) The most useful layers for classifying true/false statements seem to be consistently around layer 10-15 no matter what sparsity is.

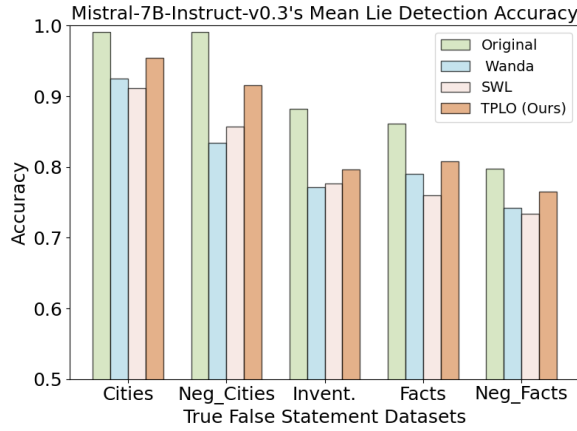


Figure 8: The visualization of the impact of 50% sparsity (via Wanda, SWL, and TPLO) on Mistral-7B-Instruct-v0.3's probing (lie detection) accuracy across several true false datasets via logistic regression.

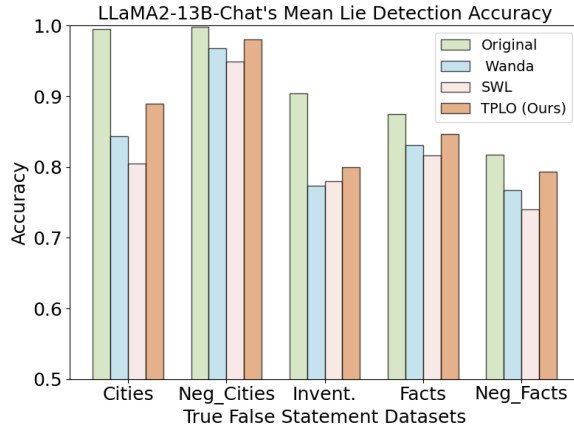


Figure 9: The visualization of the impact of 50% sparsity (via Wanda, SWL, and TPLO) on LLaMA3.1-8B-Instruct's probing (lie detection) accuracy across several true false datasets via logistic regression.

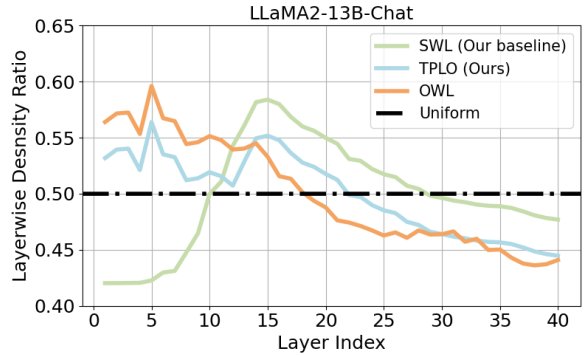


Figure 11: The visualization of the SWL layer-wise density (Our baseline), TPLO layer-wise density (Ours), OWL layer-wise density, and uniform layer-wise density at 50% sparsity, where density = 1 - sparsity.

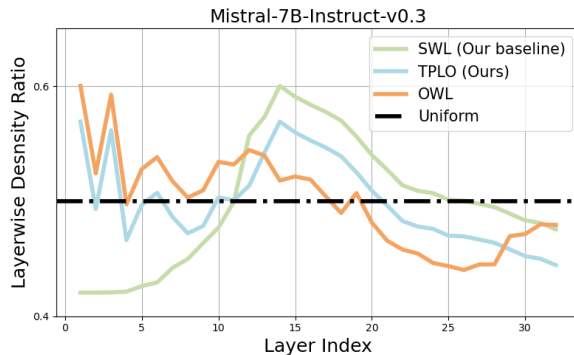


Figure 10: The visualization of the SWL layer-wise density (Our baseline), TPLO layer-wise density (Ours), OWL layer-wise density, and uniform layer-wise density at 50% sparsity, where density = 1 - sparsity.

Methods	Calibration Data	Perplexity ↓	Cities	Neg_Cities	Invent.	Facts	Neg_Facts	Average
Original-LR	N/A	6.10	0.9951	0.9986	0.9046	0.8746	0.8172	0.9421±0.0068
Wanda-LR	C4	7.50	0.8439	0.9680	0.7737	0.8313	0.7671	0.8716±0.0202
Wanda-LR	C4 + ETruthQA	7.55	0.7916	0.9554	0.7786	0.8126	0.7599	0.8627±0.0186
OWL-LR	C4	7.69	0.8355	0.9703	0.7864	0.8327	0.7754	0.8761±0.0167
OWL-LR	C4 + ETruthQA	7.78	0.8795	0.9776	0.7812	0.8374	0.7951	0.8890±0.0139
SWL-LR	C4	7.81	0.8046	0.9492	0.7800	0.8169	0.7402	0.8628±0.0205
SWL-LR	C4 + enrichedTruthQA	7.62	0.6845	0.9566	0.7571	0.7967	0.7437	0.8454±0.0166
TPLO-LR	C4	7.65	0.8871	0.9765	0.8001	0.8399	0.7856	0.8852±0.0032
TPLO-LR	C4 + ETruthQA	7.71	0.8897	0.9802	0.7997	0.8469	0.7936	0.8992±0.0148
Original-CCS	N/A	6.10	0.8296	0.8218	0.8096	0.8087	0.7040	0.8239±0.0781
Wanda-CCS	C4	7.50	0.6961	0.7646	0.5561	0.6420	0.6154	0.6655±0.0801
Wanda-CCS	C4 + ETruthQA	7.55	0.7376	0.7866	0.5530	0.7304	0.6600	0.7026±0.0681
OWL-CCS	C4	7.69	0.7468	0.8203	0.5962	0.7164	0.6487	0.7082±0.0793
OWL-CCS	C4 + ETruthQA	7.78	0.7214	0.8656	0.5830	0.7240	0.6620	0.7119±0.0644
SWL-CCS	C4	7.81	0.6707	0.7650	0.5146	0.6421	0.6081	0.6590±0.0568
SWL-CCS	C4 + ETruthQA	7.62	0.7067	0.8064	0.5114	0.6639	0.6327	0.6597±0.0743
TPLO-CCS	C4	7.65	0.7484	0.8633	0.6079	0.7205	0.6701	0.7103±0.0122
TPLO-CCS	C4 + ETruthQA	7.71	0.7554	0.8783	0.5941	0.7311	0.6749	0.7283±0.0692
Original-MM	N/A	6.10	0.9284	0.9978	0.8374	0.8085	0.7214	0.8761±0.0066
Wanda-MM	C4	7.50	0.5835	0.9737	0.7349	0.7948	0.6398	0.7993±0.0160
Wanda-MM	C4 + ETruthQA	7.55	0.6105	0.9644	0.7445	0.7900	0.6357	0.7999±0.0115
OWL-MM	C4	7.69	0.6140	0.9702	0.7620	0.7897	0.6532	0.8088±0.0106
OWL-MM	C4 + ETruthQA	7.78	0.6209	0.9609	0.7621	0.7887	0.6570	0.8025±0.0115
SWL-MM	C4	7.81	0.5522	0.9508	0.7349	0.7643	0.6198	0.7792±0.0102
SWL-MM	C4 + ETruthQA	7.62	0.5743	0.9204	0.7140	0.7534	0.6216	0.7728±0.0096
TPLO-MM	C4	7.65	0.6351	0.9725	0.7649	0.7991	0.6583	0.8202±0.0102
TPLO-MM	C4 + ETruthQA	7.71	0.6359	0.9848	0.7750	0.8034	0.6683	0.8222±0.0136
Original-TTPD	N/A	6.10	0.9746	0.9996	0.9142	0.8624	0.7502	0.9351±0.0026
Wanda-TTPD	C4	7.50	0.7236	0.9750	0.6891	0.8669	0.6978	0.8762±0.0032
Wanda-TTPD	C4 + ETruthQA	7.55	0.7582	0.9735	0.7332	0.8604	0.6868	0.8760±0.0039
OWL-TTPD	C4	7.69	0.541	0.9874	0.7337	0.8556	0.7104	0.8841±0.0045
OWL-TTPD	C4 + ETruthQA	7.78	0.7572	0.9867	0.7543	0.8520	0.7158	0.8887±0.0025
SWL-TTPD	C4	7.81	0.6396	0.9542	0.7178	0.8561	0.6777	0.8579±0.0036
SWL-TTPD	C4 + ETruthQA	7.62	0.7069	0.9595	0.7116	0.8606	0.6885	0.8692±0.0043
TPLO-TTPD	C4	7.65	0.7531	0.9901	0.7601	0.8774	0.7157	0.8716±0.0021
TPLO-TTPD	C4 + ETruthQA	7.71	0.7691	0.9951	0.7797	0.8674	0.7204	0.8846±0.0037

Table 4: The experimental results on the True-False dataset using LLaMA2-13B-Chat. "Average" means average probing accuracies on 12 True-False datasets ("cities", "neg_cities", "sp_en_trans", "neg_sp_en_trans", "inventors", "neg_inventors", "animal_class", "neg_animal_class", "element_symb", "neg_element_symb", "facts", "neg_facts").

Methods	Calibration Data	Perplexity ↓	Cities	Neg_Cities	Invent.	Facts	Neg_Facts	Average
Original-LR	N/A	5.89	0.9911	0.9909	0.8826	0.8609	0.7977	0.9293±0.0107
Wanda-LR	C4	7.36	0.9251	0.8344	0.7710	0.7901	0.7423	0.8458±0.0154
Wanda-LR	C4 + ETruthQA	7.23	0.9335	0.8096	0.7645	0.7785	0.7304	0.8417±0.0190
OWL-LR	C4	7.26	0.9476	0.8710	0.7779	0.7958	0.7475	0.8478±0.0124
OWL-LR	C4 + ETruthQA	7.35	0.9483	0.9022	0.7849	0.8028	0.7540	0.8551±0.0135
SWL-LR	C4	7.41	0.9360	0.8602	0.7766	0.7844	0.7156	0.8198±0.0196
SWL-LR	C4 + ETruthQA	7.45	0.9445	0.8990	0.7709	0.7918	0.7041	0.8254±0.0167
TPLO-LR	C4	7.32	0.9545	0.9059	0.7968	0.8013	0.7653	0.8604±0.0031
TPLO-LR	C4 + ETruthQA	7.38	0.9541	0.9160	0.7901	0.8081	0.7612	0.8647±0.0161
Original-CCS	N/A	5.89	0.7738	0.7806	0.6766	0.7707	0.7261	0.7973±0.0633
Wanda-CCS	C4	7.36	0.6832	0.7033	0.5199	0.6636	0.6112	0.6151±0.0460
Wanda-CCS	C4 + ETruthQA	7.23	0.6553	0.6855	0.5656	0.5912	0.5391	0.6327±0.0645
OWL-CCS	C4	7.26	0.7807	0.7767	0.6080	0.6353	0.5786	0.6785±0.0669
OWL-CCS	C4 + ETruthQA	7.35	0.7735	0.7641	0.6014	0.6721	0.6254	0.6875±0.0756
SWL-CCS	C4	7.41	0.6598	0.6555	0.5045	0.5963	0.5608	0.5824±0.0509
SWL-CCS	C4 + ETruthQA	7.45	0.6475	0.6257	0.5381	0.5806	0.5256	0.5736±0.0424
TPLO-CCS	C4	7.32	0.8001	0.7901	0.6201	0.7313	0.6651	0.6901±0.0312
TPLO-CCS	C4 + ETruthQA	7.38	0.7909	0.7925	0.6256	0.7423	0.6701	0.6995±0.0733
Original-MM	N/A	5.89	0.9421	0.9957	0.7748	0.8612	0.7051	0.9051±0.0037
Wanda-MM	C4	7.36	0.8436	0.9554	0.6902	0.8315	0.6807	0.8316±0.0141
Wanda-MM	C4 + ETruthQA	7.23	0.8617	0.9555	0.7285	0.8377	0.6913	0.8421±0.0108
OWL-MM	C4	7.26	0.8951	0.9624	0.7322	0.8445	0.6825	0.8647±0.0093
OWL-MM	C4 + ETruthQA	7.35	0.8918	0.9719	0.7011	0.8479	0.6780	0.8699±0.0102
SWL-MM	C4	7.41	0.8164	0.8792	0.6733	0.8195	0.6611	0.8005±0.0142
SWL-MM	C4 + ETruthQA	7.45	0.7963	0.8694	0.6878	0.8311	0.6742	0.8009±0.0129
TPLO-MM	C4	7.32	0.8998	0.9801	0.7401	0.8501	0.6976	0.8651±0.0013
TPLO-MM	C4 + ETruthQA	7.38	0.9001	0.9787	0.7432	0.8559	0.7076	0.8702±0.0120
Original-TTPD	N/A	5.89	0.9786	0.9875	0.8923	0.8774	0.7393	0.9311±0.0029
Wanda-TTPD	C4	7.36	0.9230	0.9652	0.6860	0.8286	0.7127	0.8705±0.0032
Wanda-TTPD	C4 + ETruthQA	7.23	0.9271	0.9602	0.7195	0.8373	0.7227	0.8722±0.0038
OWL-TTPD	C4	7.26	0.9376	0.9767	0.7539	0.8552	0.7289	0.8825±0.0043
OWL-TTPD	C4 + ETruthQA	7.35	0.9281	0.9739	0.7513	0.8529	0.7301	0.8831±0.0036
SWL-TTPD	C4	7.41	0.9070	0.9551	0.6672	0.8184	0.7090	0.8495±0.0035
SWL-TTPD	C4 + ETruthQA	7.45	0.8908	0.9568	0.6806	0.8255	0.7028	0.8477±0.0040
TPLO-TTPD	C4	7.32	0.9354	0.9731	0.7801	0.8601	0.7321	0.8874±0.0012
TPLO-TTPD	C4 + ETruthQA	7.38	0.9414	0.9790	0.7766	0.8676	0.7453	0.8915±0.0021

Table 5: The experimental results on the True-False dataset using Mistral-7B-Instruct-v0.3. "Average" means average probing accuracies on 12 True-False datasets ("cities", "neg_cities", "sp_en_trans", "neg_sp_en_trans", "inventors", "neg_inventors", "animal_class", "neg_animal_class", "element_symb", "neg_element_symb", "facts", "neg_facts").

Models	Methods	Calibration Data	MC			Open-Ended Generation		
			MC1↑	MC2↑	MC3↑	%Truth↑	%Info↑	%T*I↑
LLaMA2-13B-Chat + DoLa	Original	N/A	33.54	52.14	25.22	67.84	57.47	38.98
	Original	N/A	35.19	64.37	32.05	68.25	58.62	40.01
LLaMA2-13B-Chat + DoLa	Wanda	C4	24.13	42.27	17.11	60.13	50.25	30.21
	Wanda	C4	26.76	44.51	24.31	61.58	51.63	31.79
LLaMA2-13B-Chat + DoLa	Wanda	C4 + ETruthQA	25.21	43.34	18.36	61.11	51.38	31.39
	Wanda	C4 + ETruthQA	27.45	45.71	25.89	62.25	52.65	32.77
LLaMA2-13B-Chat + DoLa	OWL	C4	24.01	42.12	17.05	60.14	50.01	30.07
	OWL	C4	26.67	44.54	24.78	61.65	51.78	31.92
LLaMA2-13B-Chat + DoLa	OWL	C4 + ETruthQA	25.11	43.56	18.51	61.03	51.16	31.22
	OWL	C4 + ETruthQA	27.65	45.78	25.85	62.56	52.78	33.02
LLaMA2-13B-Chat + DoLa	TPLO (Ours)	C4	24.57	43.78	18.89	60.69	51.87	31.48
	TPLO (Ours)	C4	26.91	46.01	27.32	61.88	52.91	32.74
LLaMA2-13B-Chat + DoLa	TPLO (Ours)	C4 + ETruthQA	25.78	44.81	19.91	61.52	52.35	32.21
	TPLO (Ours)	C4 + ETruthQA	27.81	46.93	26.54	62.91	53.65	33.75

Table 6: Experimental results on TruthfulQA (Lin et al., 2021): 1) multiple choice tasks (MC1, MC2, and MC3); and 2) open-ended generation tasks, where %T*I stands for %Truth*%Info. We could see that pruning at 50% sparsity will degrade LLMs’ performance on TruthfulQA and utilizing DoLa (Chuang et al., 2023) can mitigate this degradation.

Models	Methods	Calibration Data	MC			Open-Ended Generation		
			MC1↑	MC2↑	MC3↑	%Truth↑	%Info↑	%T*I↑
LLaMA3.1-8B-Instruct + DoLa	Original	N/A	38.61	58.70	30.45	60.11	27.46	16.51
	Original	N/A	37.08	66.48	34.83	64.05	37.59	24.07
LLaMA3.1-8B-Instruct + DoLa	Wanda	C4	29.18	48.81	22.77	55.13	23.65	13.03
	Wanda	C4	30.13	56.24	30.15	59.21	33.67	19.93
LLaMA3.1-8B-Instruct + DoLa	Wanda	C4 + ETruthQA	30.22	50.01	23.95	56.41	24.21	13.66
	Wanda	C4 + ETruthQA	30.01	58.14	31.27	60.31	34.55	20.84
LLaMA3.1-8B-Instruct + DoLa	OWL	C4	29.01	48.13	22.24	55.01	23.25	12.79
	OWL	C4	30.15	56.24	30.67	59.13	33.02	19.52
LLaMA3.1-8B-Instruct + DoLa	OWL	C4 + ETruthQA	30.11	50.01	24.01	56.12	24.09	13.52
	OWL	C4 + ETruthQA	30.98	58.32	32.36	60.03	34.21	20.54
LLaMA3.1-8B-Instruct + DoLa	TPLO	C4	29.49	49.55	23.63	57.01	24.89	14.19
	TPLO	C4	29.01	57.31	30.89	60.21	34.41	21.06
LLaMA3.1-8B-Instruct + DoLa	TPLO	C4 + ETruthQA	30.81	50.74	24.95	57.89	25.42	14.72
	TPLO	C4 + ETruthQA	32.15	58.17	32.35	61.52	35.91	21.66

Table 7: Experimental results on TruthfulQA (Lin et al., 2021): 1) multiple choice tasks (MC1, MC2, and MC3); and 2) open-ended generation tasks, where %T*I stands for %Truth*%Info. We could see that pruning at 50% sparsity will degrade LLMs’ performance on TruthfulQA and utilizing DoLa (Chuang et al., 2023) can mitigate this degradation.

Models	Perplexity	Probe on Cities	Probe on Neg_Cities
Original	6.10	0.9951	0.9986
Wanda of 0.4 sparsity	7.01	0.8825	0.9701
TPLO of 0.4 sparsity	7.12	0.9213	0.9723
Wanda of 0.5 sparsity	7.50	0.8439	0.9680
TPLO of 0.5 sparsity	7.65	0.8871	0.9765
Wanda of 0.6 sparsity	8.21	0.8124	0.9011
TPLO of 0.6 sparsity	8.13	0.8321	0.9139
Wanda of 0.65 sparsity	9.32	0.7631	0.8347
TPLO of 0.65 sparsity	9.25	0.7912	0.8531

Table 8: Experimental results on the relationship between lie detection accuracy (across city topics) and perplexity for LLaMA2-13B-Chat (LR, C4). As shown, TPLO achieves comparable perplexity to Wanda, while offering improved lie detection capabilities.

Models	Perplexity	Probe on Cities	Probe on Neg_Cities
Original	8.28	0.9892	0.9942
Wanda of 0.4 sparsity	10.14	0.9013	0.7325
TPLO of 0.4 sparsity	10.21	0.9431	0.7851
Wanda of 0.5 sparsity	11.97	0.8968	0.7215
TPLO of 0.5 sparsity	11.91	0.9254	0.7661
Wanda of 0.6 sparsity	12.56	0.8541	0.6881
TPLO of 0.6 sparsity	12.32	0.8951	0.7221
Wanda of 0.65 sparsity	14.21	0.8154	0.6321
TPLO of 0.65 sparsity	14.25	0.8431	0.6657

Table 9: Experimental results on the relationship between lie detection accuracy (across city topics) and perplexity for LLaMA3.1-8B-Instruct (LR, C4). As shown, TPLO achieves comparable perplexity to Wanda, while offering improved lie detection capabilities.